

<https://doi.org/10.1038/s41541-025-01193-y>

A new attenuated and highly immunogenic orthopoxvirus vaccine protects against mpox in mice and macaques

Check for updates

Fengwen Xu^{1,4}, Yu Huang^{1,4}, Yongzhi Hou^{2,4}, Yu Xie^{1,4}, Baoying Huang^{3,4}, Fei Zhao^{1,4}, Zhao Gao¹, Chen Chen¹, Jiaxun Wang¹, Shan Mei¹, Yamei Hu¹, Liming Wang¹, Liang Wei¹, Jingjing Zhang², Na Li², Zhe Cong², Jianrong Ma², Lin Zhu², Ting Chen², Jiahua Lu², Qiang Wei², Wenjie Tan³✉, Jing Xue²✉ & Fei Guo¹✉

Shortly after 2022, mpox again becomes a public health emergency of international concern as declared by the World Health Organization on August 14, 2024. Smallpox vaccines ACAM2000 and MVA-BN were approved for mpox prevention in several countries. However, the side effects of ACAM2000 and the limited supply of MVA call for the development of new mpox vaccines to prevent mpox and other orthopoxvirus infections. In this study, we engineered a new generation of attenuated and highly immunogenic vaccinia virus named dBTF based on the vaccinia Tiantan strain which is a replication-competent smallpox vaccine widely used in China. The dBTF vaccinia virus is impaired in replication and low in virulence, induces strong vaccinia virus-specific humoral and cellular immune responses. Importantly, single dose of dBTF vaccination effectively protects mice and cynomolgus macaques from mpox virus challenge. These results support the development of dBTF into a new generation of mpox and orthopoxvirus vaccines.

Since the outbreak of monkeypox (mpox) in May 2022, as of June 30, 2024, mpox has spread to 116 countries and regions worldwide, with 99,176 reported cases and 208 deaths¹. The World Health Organization (WHO) previously declared the spread of mpox as a global health emergency in July 2022 which ended in May 2023. With the new mpox outbreaks caused by clade I viruses, the WHO made the same declaration on August 14, 2024, highlighting the grave public threat by mpox and the urgent need of vaccines and treatments to mitigate mpox. Mpox viruses (MPXVs) are classified into two genetic clades, I and II. The clade II MPXV was responsible for the global outbreak in 2022. The clade I MPXV caused the ongoing outbreak in Africa in 2024, and has spread into other countries including Sweden and Thailand. With the limited number of mpox drugs, vaccination remains the best way to prevent and control mpox spread².

Smallpox vaccines have shown efficacy in protecting against mpox because of the high sequence conservation among orthopoxviruses^{3–8}.

Smallpox vaccines have undergone several upgrades^{9,10}. The first generation of smallpox vaccines is live vaccinia strains including the New York City Board of Health (NYCBH) strain, the Lister strain, and the Temple of Heaven (Tiantan) strain¹¹. These smallpox vaccines played important roles in the Eradication Campaign against smallpox; however, their use is associated with a number of severe side effects such as vaccine-related myocarditis, myopericarditis, vaccinia necrosum, generalised vaccinia, and eczema vaccinatum^{12,13}. As an effort to control possible microbial contamination and allergenic animal proteins, the second generation of smallpox vaccines was produced with tissue culture systems or embryonated chicken eggs, which mainly include ACAM1000, ACAM2000, and Elstree-BN. These vaccines are replication-competent viruses and still cause adverse events such as myocarditis and pericarditis^{14,15}. The third-generation of smallpox vaccines was developed by serial passages of a parental vaccine strain for further attenuation; these include MVA, LC16m8,

¹Key Laboratory of Pathogen Infection Prevention and Control (Ministry of Education), State Key Laboratory of Respiratory Health and Multimorbidity, National Institute of Pathogen Biology, Chinese Academy of Medical Sciences & Peking Union Medical College, Beijing, China. ²State Key Laboratory of Respiratory Health and Multimorbidity, NHC Key Laboratory of Human Disease Comparative Medicine, Beijing Key Laboratory for Animal Models of Emerging and Reemerging Infectious Diseases, Institute of Laboratory Animal Science, Chinese Academy of Medical Sciences and Peking Union Medical College, Beijing, China. ³NHC Key Laboratory of Biosafety, National Key Laboratory of Intelligent Tracking and Forecasting for Infectious Diseases, National Institute for Viral Disease Control and Prevention, Chinese Center for Disease Control and Prevention, Beijing, China. ⁴These authors contributed equally: Fengwen Xu, Yu Huang, Yongzhi Hou, Yu Xie, Baoying Huang, Fei Zhao. ✉e-mail: tanwj@ivdc.chinacdc; xuejing@cnilas.org; guofei@ipb.pumc.edu.cn

NYVAC^{16–18}. MVA is a highly attenuated and replication-deficient strain, demonstrates the highest safety profile, but requires high inoculation amount or multiple doses to generate effective immune protection, compared with the other smallpox vaccines^{19–22}. ACAM2000 and MVA-BN (JYNNEOS, IMVANEX, and IMVAMUNE) have been approved for mpox prevention in several countries^{23,24}. MVA-BN is more recommended because of its better safety profile compared with ACAM2000. The real-world efficacy of MVA-BN against mpox is 72.1% protection for 1 dose and 87.8% protection for 2 doses among immunocompetent participants, and 51.0% protection for 1 dose and 70.2% protection for 2 doses among immunocompromised participants²⁵. However, the supply of MVA-BN vaccine is rather limited. As of August 2024, Africa countries require 10 million doses of mpox vaccines, while only 200,000 doses of MVA-BN are currently available²⁶. With the frequent mpox outbreaks and the shortage of safe and effective mpox vaccines²⁷, the development of new mpox vaccines is warranted.

Vaccinia Tiantan strain (VTT) is replication competent and was widely used in China during the global smallpox eradication campaign, but it does induce severe side effects in some vaccinees^{28,29}. Although the incidence is relatively low, the VTT vaccine still needs to be improved to increase its safety. To improve the safety of VTT, modifications have been made in the process of developing VTT into a viral vector. Deletion of *J2R*, the gene encoding for viral thymidine kinase (TK), was one of the most common strategies to generate attenuated vaccinia virus^{30–32}. TK deletion diminishes viral virulence in mice and rhesus macaques^{33,34}. In addition, the small subunit of the heterodimeric ribonucleoside diphosphate reductase complex (*F4L*) is an important virulence factor. *F4L* deletion reduces the yield of vaccinia virus up to 1000 folds in cells, and severely attenuates the virus in mice³⁵. To generate an attenuated VTT strain that serves as a safer poxvirus vaccine, we deleted the *TK* and *F4L* genes both of which regulate deoxynucleoside triphosphate (dNTP) production during viral DNA replication^{36,37}. However, the attenuation of live vaccinees is often accompanied with low immunogenicity. MVA lost about 15% of the parental CVA genome during serial passages, and these large deletions lead to high attenuation but also compromise immunogenicity^{38,39}. High immunization dose and the prime-boost regimen for MVA are required to generate protective immunity. In this study, to maintain the high immunogenicity which often diminishes concomitant with reduction in virulence, we deleted the *B2R* gene which encodes an innate immune regulator blocking cGAS/STING pathway activation^{40,41}, along with *TK* and *F4L*. This *TK*, *F4L*, and *B2R* triple-gene-deleted virus is called dBTF, which is impaired in its replication in mammalian cells, less virulent in vivo, and maintains high immunogenicity. Importantly, immunization with dBTF protects mice and cynomolgus macaques from MPXV challenge, supporting the utility of dBTF as a safe and effective mpox and orthopoxvirus vaccine.

Results

Construction of an attenuated and highly immunogenic vaccinia virus

To reduce the virulence and increase the immunogenicity of VTT, several recombinant viruses with gene deletions were generated. To improve the safety profile of VTT, two viral genes *J2R* (*TK*) and *F4L* were deleted either individually or in combination, giving rise to dTK, dF4L, and dTF. Both genes encode enzymes regulating nucleotide metabolism, with *J2R* (*TK*) encoding the thymidine kinase and *F4L* encoding the small subunit of the ribonucleotide reductase complex. To compensate for the decrease in immunogenicity caused by attenuation, the *B2R* gene was deleted to produce dB2R or dBTF with deletion of triple genes *TK/F4L/B2R* (Fig. 1A). *B2R* was chosen for deletion because it encodes poxin protein that blocks cGAS/STING pathway activation. All recombinant viruses were verified by PCR and sequencing (Fig. S1A). To examine the replication capacity of these viruses in mammalian cells, the growth kinetics of VTT, dTK, dF4L, dTF, dB2R, and dBTF were monitored in BSC-40 and LO2 cells. The triple deletion virus dBTF exhibited the slowest replication kinetics, followed by

the double deletion virus dTF, and the three single deletion viruses (Fig. 1B). Consistent with their significant reduction in virus replication, the dBTF and dTF viruses formed much smaller plaques compared with wild type VTT (Fig. 1C). To evaluate the genetic stability of these deletion viruses, we serially passaged the viruses in Vero cells. The consistency of passage 0, passage 5, and passage 10 of these viruses was verified by PCR and sequencing, and each generation of these viruses propagated at similar levels and exhibited similar plaque phenotypes (Fig. S1B–S1C). Since *B2R* cleaves 2',3'-cGAMP and prevents the activation of cGAS/STING pathway, wild type VTT and the mutants dTK, dF4L, and dTF effectively suppressed the production of cGAMP, phosphorylation of IRF3 and TBK1, and the expression of IFN- β and ISG56 (Fig. 1D–F), as opposed to the dB2R and dBTF mutants, of which the infection activated cGAS, downstream IRF3/TBK1 signaling, and IFN- β production (Fig. 1D–F). Together, these data demonstrate that dBTF is significantly reduced in its replication in vitro, while its infection induces innate immune response.

Assessment of in vivo attenuation of the triple deletion virus dBTF

We first compared the virulence of wild type VTT and its deletion mutants dTK, dF4L, dTF, dB2R, and dBTF in rabbits that were intradermally inoculated. The sizes of erythema at inoculation sites were measured. At the inoculation dose of 10^5 PFU, the double deletion mutant dTF and the triple deletion mutant dBTF caused lesions three times smaller than those caused by the wild type VTT. Among the three single deletion mutants, dB2R inoculation caused lesions of the same size as by the wild type VTT, whereas dTK and dF4L inflicted lesions two times smaller than those by VTT. At the inoculation dose of 10^4 PFU, lesions caused by dTF and dBTF were resolved 8 days after inoculation (Figs. 2A, S2A).

We next examined the pathogenicity of these recombinant viruses in BALB/c mice. Intranasal inoculation of VTT and dB2R led to significant weight loss of mice, with the fatality rate of 80% (4/5), 40% (2/5) at the dose of 2.5×10^5 PFU, and 100% (5/5), 100% (5/5) at the dose of 2.5×10^6 PFU (Fig. 2B, D). Mice survived infection by dTK, dF4L, dTF, or dBTF at both doses of 2.5×10^5 PFU and 2.5×10^6 PFU (Fig. 2B, D). Viral loads in the lungs, brains, hearts, spleens, kidneys, and livers of mice infected with dTF or dBTF viruses decreased significantly compared with VTT on 4 d.p.i. (Figs. 2C, E, S2B–S2C). These results showed that dTF and dBTF were highly attenuated in mice.

To evaluate the neurovirulence of these mutants, an inoculum of 10^5 PFU was intracranially inoculated in BALB/c mice. 40% mice survived VTT infection, while all mice survived the infection by each virus mutant, with no weight loss in the dTF and dBTF group (Fig. 3A, B). The viral loads in the brains of dTF and dBTF-infected mice were the lowest on 4 d.p.i. among all viruses tested (Figs. 3C, S2D).

Lastly, we evaluated the virulence of these VTT mutants in nude mice as an immune compromised animal model. Similar to the phenotypes in BALB/c mice, VTT and dB2R inoculation led to 100% or 80% death, while all nude mice survived infection by dTK, dF4L, dTF, or dBTF (Fig. 3D, E). Significant decreases in viral loads were observed in the tissues of mice infected by dTF and dBTF compared with VTT (Figs. 3F, S2E). Together, these in vivo data demonstrate that the dTF and dBTF present markedly reduced virulence and neurovirulence.

Low-dose inoculation of dBTF elicits protective immunity against vaccinia virus infection in mice

We further assessed the immunogenicity and protection efficacy of these deletion mutants against vaccinia virus in mice. BALB/c mice were intramuscularly inoculated twice (prime and boost) at a three-week interval with VTT, dTK, dF4L, dTF, or dBTF (Fig. S3A), and vaccinia virus-specific humoral and cellular immune responses were measured. A low (10^4 PFU) and a high (10^5 PFU) inoculation dose were tested. Although the triple deletion mutant dBTF is attenuated, it was still effective in inducing the binding antibodies 2 weeks after prime (Fig. S3B) or boost (Fig. S3C) and the VACV-neutralizing antibodies 2 weeks after boost (Fig. S3D), as well as in eliciting vaccinia virus-specific T cell responses as determined by the IFN- γ

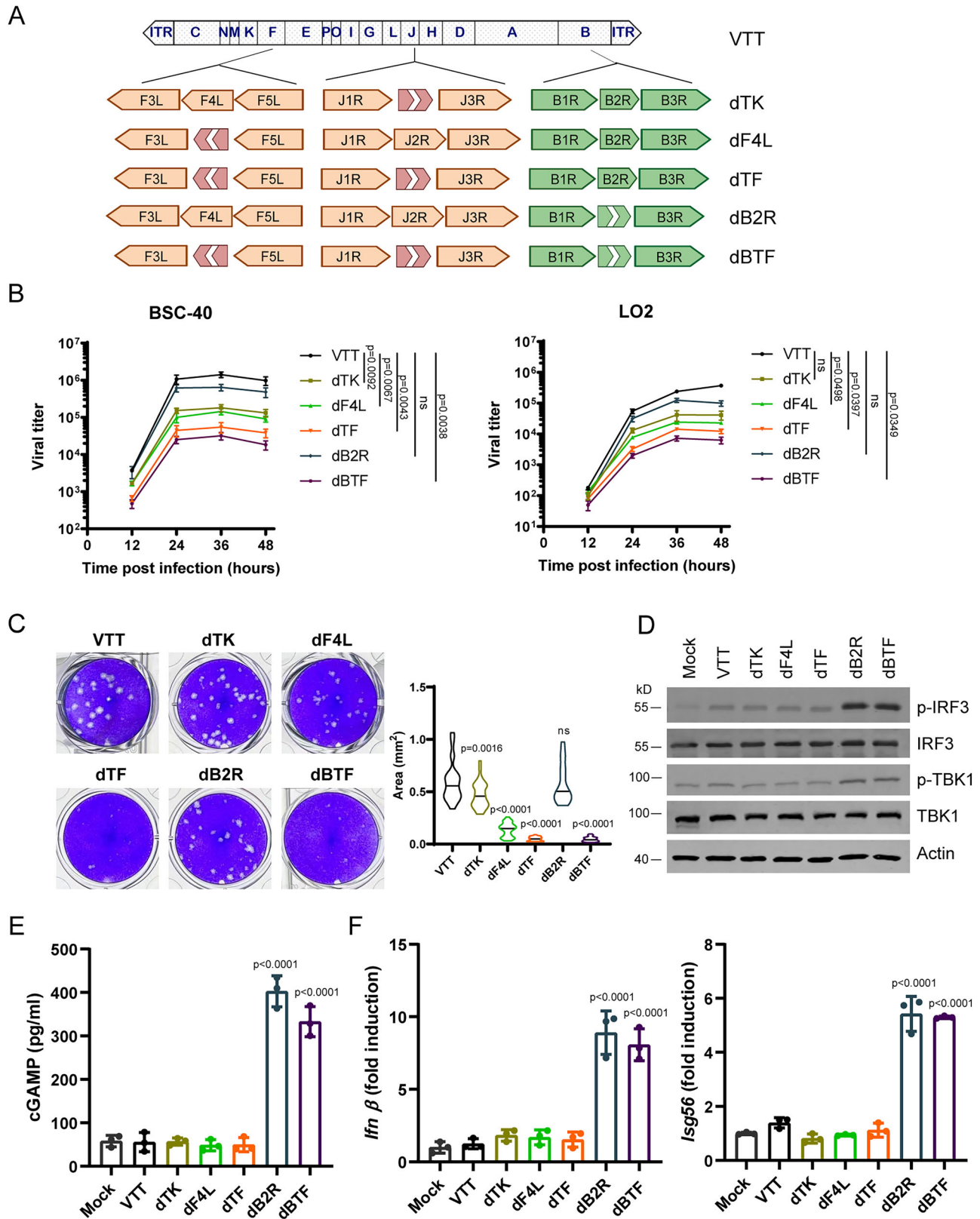


Fig. 1 | Construction of an attenuated and highly immunogenic vaccinia virus. **A** Schematic representation of recombinant viruses. **B** The replication kinetics of recombinant viruses in BSC-40 and LO2 cells ($n = 3$ biological replicates). **C** Plaque formation by recombinant viruses. **D** IRF3 and TBK1 activation in dB2R- and dBTF-infected cells. **E** Increased level of cGAMP in dB2R- and dBTF-infected cells ($n = 3$

biological replicates). **F** Increased mRNA level of *Ifn β* and *Isg56* in dB2R- and dBTF-infected cells ($n = 3$ biological replicates). Data are represented as mean \pm SD, and statistical differences are determined by one-way ANOVA with multiple comparison tests.

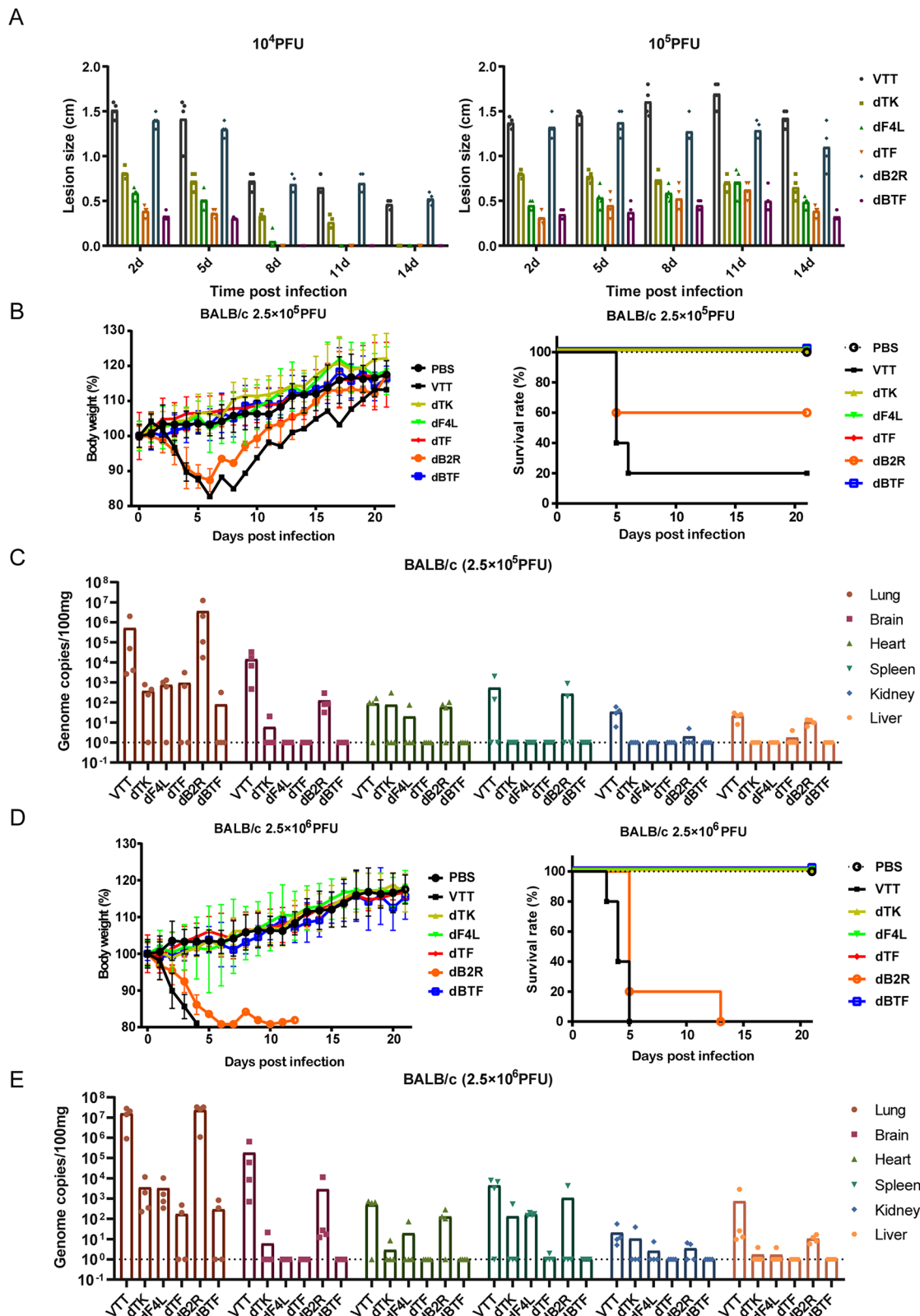


Fig. 2 | In vivo attenuation of the triple-deletion virus dBTF. **A** The sizes of erythemas induced by intradermal inoculation of viruses on rabbit backs ($n = 4$). **B, C** The body weight changes, survival rates ($n = 5$ mice) (**B**) and viral loads in the tissues ($n = 4$ mice) (**C**) of BALB/c mice intranasally inoculated with 2.5×10^5 PFU of

viruses. **D, E** The body weight changes, survival rates ($n = 5$ mice) (**D**) and viral loads in the tissues ($n = 4$ mice) (**E**) of BALB/c mice intranasally inoculated with 2.5×10^6 PFU of viruses.

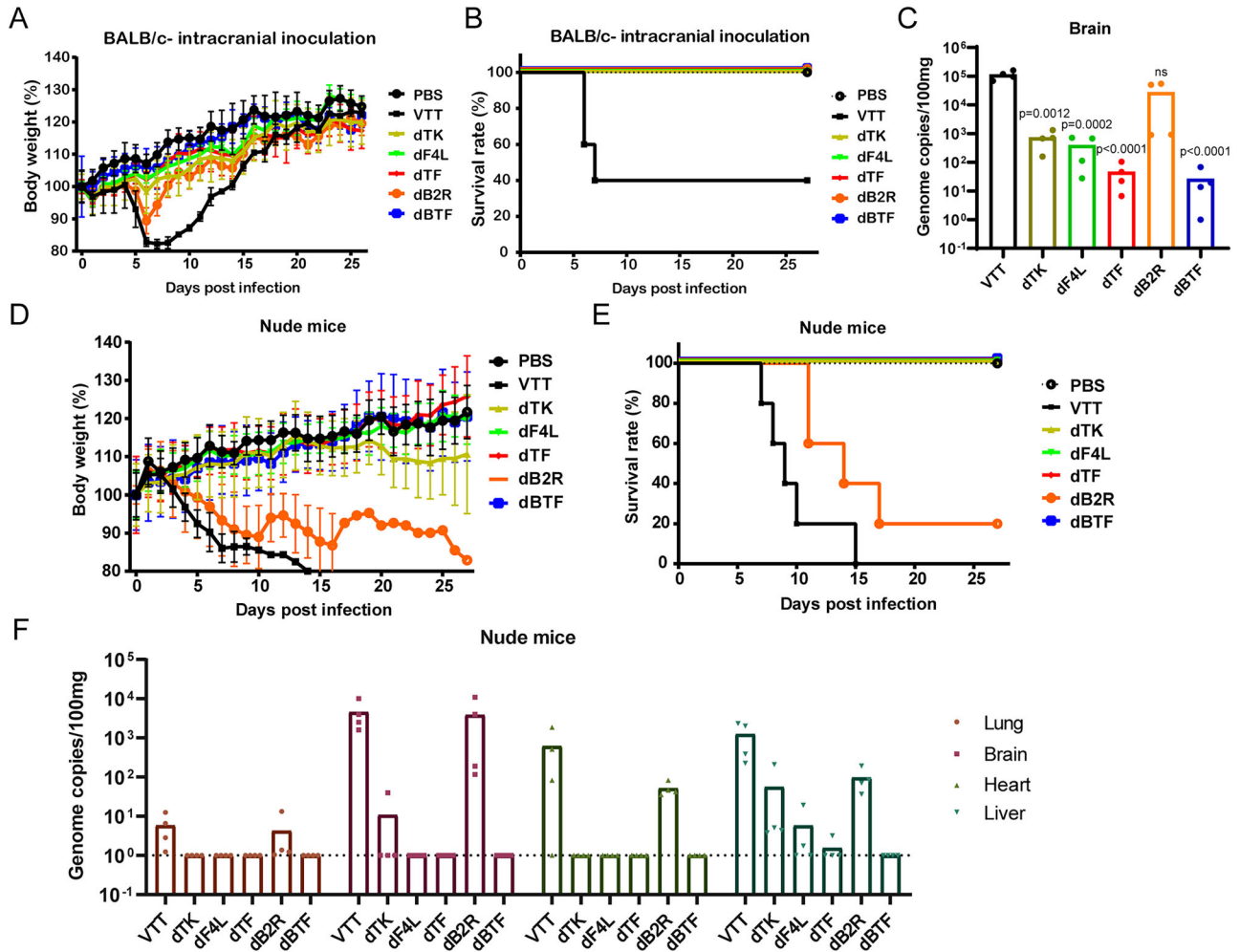


Fig. 3 | Reduced neurovirulence of the attenuated virus dBTF. A–C The body weight changes ($n = 5$ mice) (A), survival rate ($n = 5$ mice) (B), and viral loads in the brains ($n = 4$ mice) (C) of BALB/c mice intracranially inoculated with 1×10^5 PFU of viruses. D–F The body weight changes ($n = 5$ mice), survival rates ($n = 5$ mice) (E), and viral loads in the tissues ($n = 4$ mice) (F) of BALB/c nude mice intranasally inoculated with 2.5×10^5 PFU of viruses.

ELISPOT assay (Fig. S3E). The dBTF elicited slightly lower level of binding antibodies comparing to some of the VTT and the dTK groups as labeled in Figs. S3B, S3C, while there were no significant differences between dBTF and other mutants in most of the experiments (not labeled). Two weeks after boost, mice were challenged intranasally with VTT of 2.5×10^5 PFU. 80% mice in PBS group succumbed after challenge, while dBTF protected all mice as well as the other deletion mutants did (Fig. S3F).

We next tested the protection effect of the single dose inoculation with the VTT mutants on the lethal challenge of mice by the wild type VTT (Fig. 4A). The results showed that all of the deletion mutants elicited vaccinia virus-specific humoral and cellular immune responses (Fig. 4B–D). Since the dTF and dBTF mutants were attenuated the most, the immunogenicity of dTF and dBTF was compared. We expected higher immunogenicity of dBTF because the B2R gene, which encodes the cGAS/STING pathway inhibitor, was deleted. However, most of the antibody levels were not statistically different between the dTF and dBTF groups, although the antibodies induced by dBTF showed an increasing trend compared with dTF. The dBTF elicited slightly higher level of neutralizing antibodies than other mutants, as labeled in Fig. 4C, while there were no significant differences between them in most of the experiments (not labeled). Importantly, this single dose regimen with dBTF and other mutants completely protected mice against lethal challenge with vaccinia virus (Fig. 4E). These data demonstrate that dBTF, with its markedly reduced virulence, is still able to elicit protective immune responses against lethal challenge by vaccinia virus in mice.

Single-dose regimen with dBTF protects mice from MPXV

To test whether the dBTF mutant is able to protect against MPXV, we intramuscularly inoculated the CAST/Eij mice with 10^5 PFU of dBTF virus, followed by MPXV clade IIb (MPXV-B.1-China-C-Tan-CQ01) challenge via intraperitoneal route three weeks after immunization (Fig. 5A). This single-dose regimen with dBTF induced specific humoral immune responses against MPXV clade IIb (Fig. 5B–C), clade Ia, and clade Ib (Fig. 5D), as well as vaccinia virus-specific immune responses in CAST/Eij mice (Fig. S4A–S4C). Neither significant change in body weight nor clinical signs were observed after MPXV clade IIb challenge (Fig. S4D). Four days after challenge, MPXV infection was determined by measuring the levels of MPXV genome in plasma, hearts, livers, spleens, lungs, kidneys, brains, intestines, and stomach. Compared to the control group, the dBTF group had much lower MPXV genomes across all tissues, and lower viral titers in lungs, spleens, and kidneys (Fig. 5E, F), demonstrating efficient protection against MPXV challenge. We also tested correlations between the immune responses before challenge and plasma viral loads on day 4 after MPXV challenge. MPXV clade IIb-neutralization antibodies and M1R, B6R, H3L, A35R-specific binding antibodies were negatively correlated with levels of plasma viral genomes on day 4 (Figs. 5, S4E).

Macaques are protected from MPXV challenge by a single-dose dBTF immunization

To evaluate the protection efficacy of single-dose dBTF inoculation in an animal model that better recapitulates human mpox than mice, cynomolgus

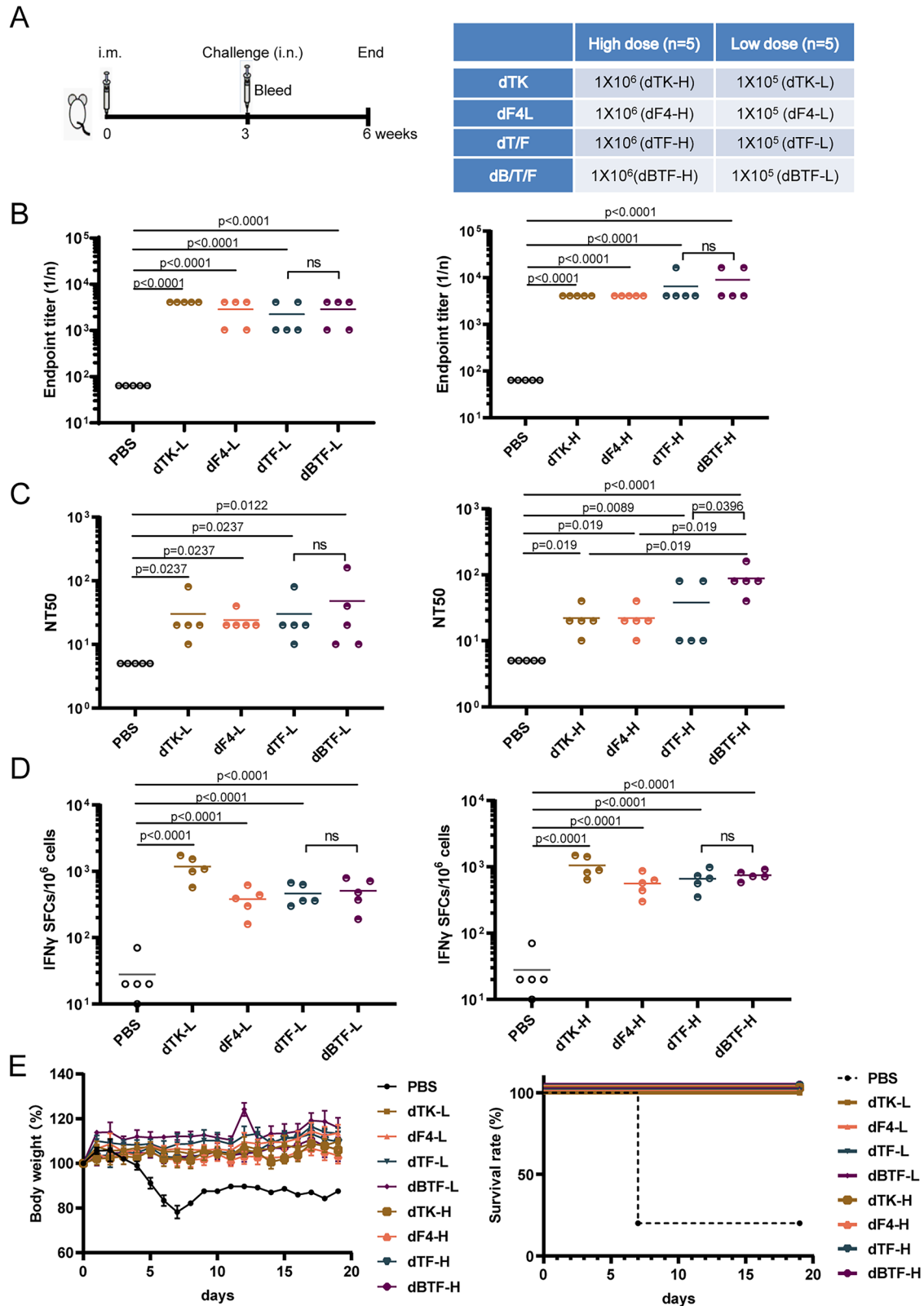


Fig. 4 | Single dose of dBTF also displays efficient protection against vaccinia virus in mice. **A** Time course of high dose (1×10^6 PFU) or low dose (1×10^5 PFU) single immunization and vaccinia virus challenge in BALB/c mice. **B** VTT-specific binding antibodies in serum of mice collected three weeks after immunization ($n = 5$ mice). **C** VTT- neutralization antibodies in serum of immunized mice ($n = 5$ mice).

D VTT-specific T cell responses in splenocytes collected three weeks after immunization ($n = 5$ mice). **E** The body weight changes and survival rates of immunized mice challenged with 2.5×10^5 PFU of vaccinia virus ($n = 5$ mice). Mean lines are shown, and statistical differences are determined by one-way ANOVA with multiple comparison tests.

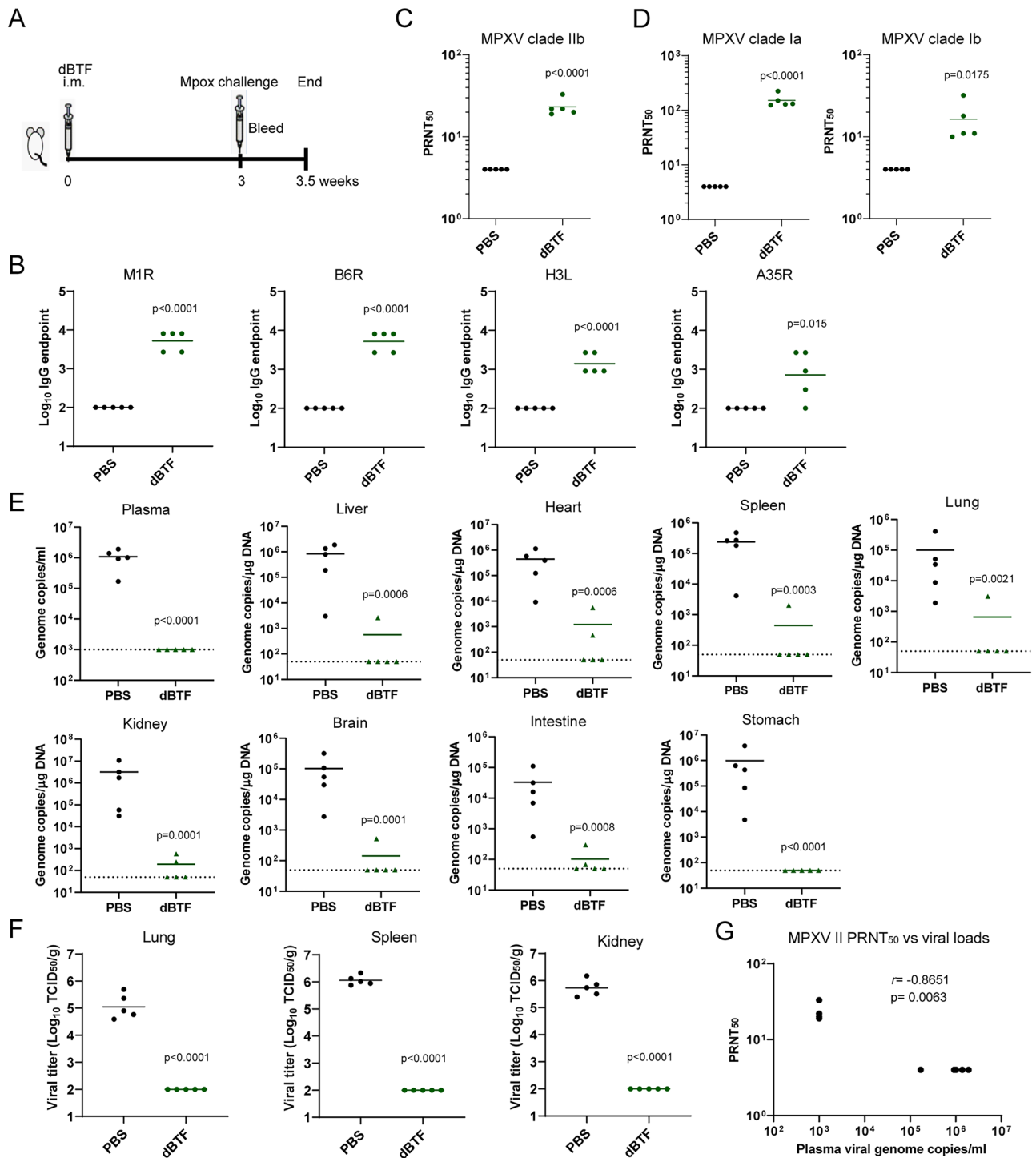


Fig. 5 | Single dose of dBTF protects mice from mpox disease. **A** CAST/Eij mice were intramuscularly vaccinated with 1×10^5 PFU dBTF, and challenged intraperitoneally with MPXV clade IIb (MPXV-B.1-China-C-Tan-CQ01) 3 weeks after inoculation. **B** MPXV M1R, B6R, H3L, A35R-specific binding antibodies in serum of mice collected three weeks after immunization ($n = 5$ mice). **C** MPXV clade IIb-neutralization antibodies in serum of immunized mice ($n = 5$ mice). **D** MPXV clade Ia (MPXV-1b-China-CDC-Tan-SD01) or MPXV clade Ib (MPXV-1b-China-CDC-

Tan-ZJ01)- neutralization antibodies in serum of immunized mice ($n = 5$ mice). **E** The viral genomes in tissues of immunized mice challenged with MPXV ($n = 5$ mice). **F** The infectious viral titers in tissues of immunized mice challenged with MPXV ($n = 5$ mice). **G** Correlations between MPXV clade IIb-neutralization antibodies and plasma viral loads. Spearman correlation coefficients (r) are reported for neutralization antibody titers with viral loads. Mean values are shown, and statistical differences are determined by two-tailed Student's t -tests.

macaques were immunized with dBTF of 2.5×10^5 PFU, followed by intravenous challenge with MPXV clade IIb (MPXV-B.1-China-C-Tan-CQ01) 28 days after immunization (Fig. 6A). Single-dose dBTF inoculation induced MPXV clade IIb and MPXV clade I-specific humoral immune responses 28 days after immunization (Fig. 6B-D). VACV-specific IgG,

neutralization antibodies, and T cell responses were also detected (Fig. S5A–S5C). In the control group, mpox skin lesions appeared on day 7 after challenge, their numbers increased to 452, 156, and 75 among the three infected macaques on day 10 (Fig. 6E). In contrast, the three macaques in the dBTF group developed 6, 5, and 1 pox lesion, respectively (Fig. 6E). Neither

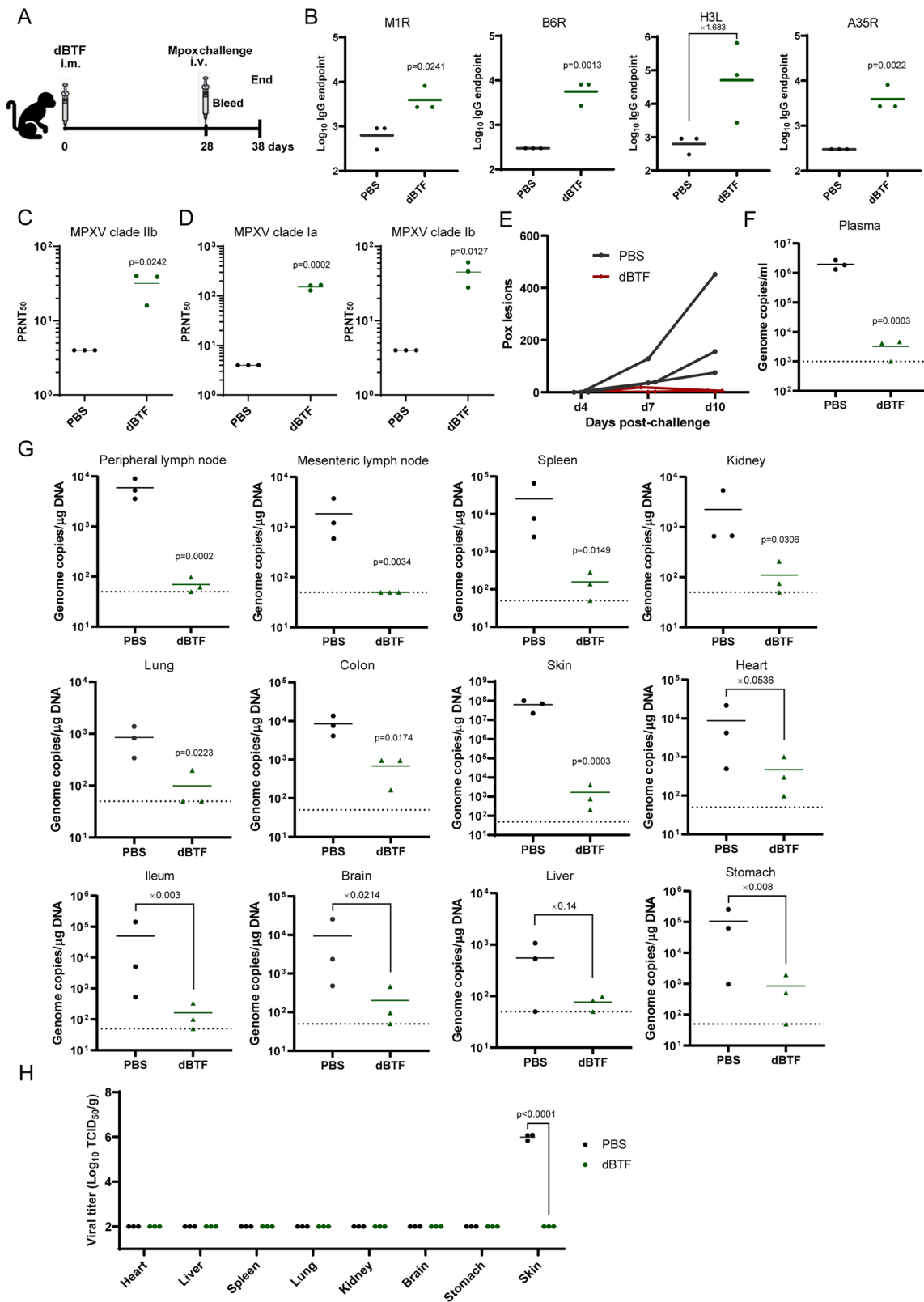


Fig. 6 | Protection of monkeys against MPXV challenge by single dose of dBTF.

A Cynomolgus macaques were intramuscularly vaccinated with 2.5×10^5 PFU dBTF, and challenged intravenously with MPXV clade IIb (MPXV-B.1-China-C-Tan-CQ01) 28 days after inoculation. **B** MPXV M1R, B6R, H3L, A35R-specific binding antibodies in serum of macaques collected 28 days after immunization ($n = 3$ macaques). **C** MPXV clade IIb- neutralization antibodies in serum of immunized animals ($n = 3$ macaques). **(D)** MPXV clade Ia, or clade Ib-

neutralization antibodies in serum of immunized animals ($n = 3$ macaques). **E** Pox lesions developed in animals 10 days after MPXV challenge. **F** The viral loads in the plasma of animals 10 days after challenge ($n = 3$ macaques). **G** Levels of viral genomes in tissues of animals 10 days after MPXV challenge ($n = 3$ macaques). **H** Levels of infectious virus in tissues of animals 10 days after MPXV challenge ($n = 3$ macaques). Mean lines are shown, and statistical differences are determined by two-tailed Student's *t*-tests.

significant change in body weight nor body temperature between the PBS control and the dBTF group was observed after challenge (Fig. S5D–S5E). MPXV viral loads in the peripheral blood and various tissues were measured, and dBTF group had markedly lower viral genomes and infectious viruses than the PBS group on day 10 after the challenge (Fig. 6G, H). M1R and H3L-specific binding antibodies were negatively correlated with levels of plasma viral genomes on day 10 (Fig. S5F). All these results demonstrate that single-dose dBTF inoculation effectively protects macaques from MPXV challenge.

Discussion

Vaccinia virus has been used as vaccine for smallpox and mpox. For example, the second-generation vaccine ACAM2000 and the third-generation vaccine MVA have been approved for mpox intervention in the 2022 mpox outbreak. However, the side effects of ACAM2000 and supply shortage of MVA call for new vaccines to prevent mpox or other orthopoxvirus infections. Vaccinia virus Tiantan (VTT) strain was widely used as a smallpox vaccine in China. It is replication-competent, eliciting strong immunity and protection against smallpox. Although VTT is less virulent than other vaccinia strains, such as WR, it remains neurovirulent²⁹. Further attenuation of VTT is thus necessary to develop a safer vaccine for MPXV and other orthopoxviruses.

Vaccinia virus is a large DNA virus. Among the many proteins vaccinia virus encodes, viral thymidine kinase enhances dTTP biogenesis. The TK deletion has been shown to reduce replication and viral virulence in vivo^{31,33,34}. However, the TK-deleted vaccinia virus is still considerably virulent in immune compromised animal models³¹. The *F4L* gene encodes for the small unit of viral ribonucleotide reductase which regulates dNTP synthesis. Virus with *F4L* deletion is highly attenuated in vivo^{35,42}. Vaccinia virus carrying deletions of both TK and *F4L* is not pathogenic in immune compromised mice³⁵. In this study, we initially generated mutants dTK, dF4L, and dTF by deleting TK and/or *F4L* to reduce the virulence of VTT. The dTF was severely impaired in its replication in mammalian cells and engendered low virulence and neurovirulence in both immunocompetent and immunocompromised mice. Then, to boost the immunogenicity which may be compromised by previous viral attenuation, we deleted the viral gene *B2R* that encodes poxin, a viral protein blocking the cGAS/STING signaling which otherwise senses viral DNA and activates the production of interferons and other cytokines. Indeed, either dB2R alone or in combination with dTF (dBTF) induced stronger innate immune responses and did not increase virulence in vivo. Vaccines ACAM2000 and MVA-BN have been approved for mpox intervention, and MVA-BN is more recommended for its safety profile. However, high immunization dose with the prime-boost regimen of MVA-BN is required for effective protection. Our triple deletion mutant dBTF is much safer and less virulent, and sufficient to protect mice and macaques from vaccinia and MPXV challenges at a single immunization with 10⁵ PFU, thus providing a competitive option of mpox vaccines. With the limited supply of MVA-BN vaccine, dBTF can be a solution to the shortage of current mpox vaccines and significantly contribute to the prevention of future MPXV and other orthopoxvirus infections.

MPXV Clade II caused the 2022 mpox outbreak, and Clade I is currently spreading among many countries. The MPXV tested in this study is Clade II, which is protected by the dBTF mutant. Although it remains to determine the protection efficacy of dBTF against Clade I MPXV, dBTF immunization induced MPXV Clade I-neutralizing antibodies (Figs. 5D, 6D), indicating the potential of dBTF in protection from Clade I MPXV. In addition to its demonstrated utility as a vaccine against smallpox, vaccinia virus possesses the oncolytic property, thus has been evaluated in cancer treatment. For example, the TK and *F4L* double-deleted virus has been reported to display tumor-selectivity replication and tumor cell killing activity³⁵. Further removal of *B2R* in the triple deletion mutant dBTF improves the safety profile and enhances viral immunogenicity, may thus exhibit greater tumor killing effect.

Methods

Viruses

Preparation of vaccinia Tiantan strain stocks and generation of recombinant viruses have been described previously⁴³. Briefly, viruses were propagated in Vero cells and purified by centrifugation through 36% sucrose cushion. Recombinant viruses dTK, dF4L, dTF, dB2R, and dBTF were constructed by homologous recombination and at least five rounds of plaque purification. The deletions of TK, *F4L*, or *B2R* in purified recombinant virus genomes were confirmed by PCR and DNA sequencing. Then the purified recombinant viruses were amplified in Vero cells, and virus titres were determined by plaque assay. Monkeypox virus (MPXV) clade IIb (MPXV-B.1-China-C-Tan-CQ01), MPXV clade Ia (MPXV-1b-China-CDC-Tan-SD01), or MPXV clade Ib (MPXV-1b-China-CDC-Tan-ZJ01) were also cultivated in Vero cells and titrated via plaque assay. All procedures were performed in a BSL-3 containment facility at the Institute of Laboratory Animal Science, Chinese Academy of Medical Sciences.

Innate immune response analysis

THP1 cells were infected with VTT, dTK, dF4L, dTF, dB2R or dBTF (MOI:1) for 6 h, then cells were harvested for immunoblotting, 2'3'-cGAMP and ISG mRNA analysis.

For immunoblotting, cell lysates were separated in a 12% SDS-PAGE gel and transferred onto nitrocellulose membranes. Membranes were blocked with 5% BSA/TBS, and incubated with following antibodies: anti-phospho IRF3 (Abcam, ab76493), anti-IRF3 (Proteintech, 11312-1-AP), anti-phospho TBK1(CST, 5483S), anti-TBK1(CST, 3013S), and anti- β -actin (Sigma-Aldrich, A1978). Then the membranes were incubated with IRDye 800-labeled IgG or IRDye 680-labeled IgG secondary antibodies, scanned with Odyssey (Li-Cor Biosciences, Lincoln, NE).

For 2'3'-cGAMP ELISA assay, 2'3'-cGAMP in the cell lysates was analyzed using the Cayman Chemical 2'3'-cGAMP ELISA Kit (501700) following the manufacturer's protocol, as previously described⁴⁴.

For analysis of ISG mRNA levels, total RNA from cells was isolated using the TRIzol reagent (Invitrogen, Carlsbad, CA, USA) according to the manufacturer's protocol. RNA was reverse transcribed into cDNA using the SuperScript III Reverse Transcriptase (Thermo Fisher) according to the manufacturer's instructions. cDNA was quantified with qRT-PCR using *Ifr* β or *Isg56* specific primers (IFN β -F: ggagcagccgcttagc, IFN β -R:tgatagacattagccaggaggttc, ISG56-F: tacagcaacctagtagtaca, ISG56-R: tcaggtgtttccatagc) and the Luna Universal qPCR Master Mix (M3003L, NEB).

Ethics statement

Animal experiments were carried out in strict accordance with the recommendations outlined in the Guide for the Care and Use of Laboratory Animals of the Ministry of Science and Technology of the People's Republic of China. All animal experiments involving infectious MPXV challenges were performed in Animal Biosafety Level 3 (ABSL-3) facilities at the Institute of Laboratory Animal Science, Chinese Academy of Medical Sciences, following the institutional biosafety manual. The rabbit experiments were approved by the Laboratory Animal Welfare and Ethics Committee of Beijing Medconn Biotechnology Co., Ltd (Approval No. MDKN-2022-091). The mice experiments were approved by the Institutional Animal Care and Use Committee (IACUC) of the Institute of Laboratory Animal Science, Chinese Academy of Medical Sciences (Approval No. XJ23002). The macaque experiments were approved by the Institutional Animal Care and Use Committee of the Institute of Laboratory Animal Science, Chinese Academy of Medical Sciences (Approval No. XJ24003).

Assessment of attenuation in vivo

New Zealand rabbits of 2.5 kg were shaved on the back and inoculated intradermally with 10⁴ or 10⁵ PFU of VTT, dTK, dF4L, dTF, dB2R, or dBTF in a volume of 50 μ L. On days 2, 5, 8, 11, and 14 post-infection, the diameters of erythema and ulcerations were measured by vernier caliper and recorded. At the end of the experiment, animals were sacrificed by intravenous injection of sodium pentobarbital at a dosage of 100 mg/kg.

To characterize virulence in mice, BALB/c mice and BALB/c nude mice were infected with different viruses. Groups of 6-week-old female BALB/c mice were infected intranasally with 2.5×10^5 or 2.5×10^6 PFU of VTT, dTK, dF4L, dTF, dB2R, and dBTF in a 25 μ L volume ($n = 9$). In each group, 5 mice were weighed daily for 21 days after infection. The remaining 4 mice were sacrificed at day 4 post-infection, and the viral loads in the tissues were determined with qRT-PCR or plaque assay.

For neurovirulence detection, groups of 5-week-old female BALB/c mice ($n = 9$) were intracranially inoculated with 1×10^3 PFU of VTT, dTK, dF4L, dTF, dB2R, or dBTF (20 μ L). In each group, 5 mice were observed daily, and survival was recorded until 28 days post infection. The remaining 4 mice were sacrificed at day 4 post-infection, the viral loads in the tissues were determined with qRT-PCR or plaque assay.

6-week-old female BALB/c nude mice were used in to characterize virulence in immunodeficient mice. Mice ($n = 9$) were challenged via the intranasal route with 2.5×10^5 PFU of VTT, dTK, dF4L, dTF, dB2R or dBTF in a 25 μ L volume. In each group, 5 mice were weighed daily for 28 days. The remaining 4 mice were sacrificed at day 4 post-infection, and the viral loads in the tissues were determined with qRT-PCR or plaque assay.

For the above mice infections, mice were anesthetized with 2% isoflurane. At the end of the experiments, mice were euthanized using 2% isoflurane, followed by cervical dislocation.

Immunization of mice and vaccinia virus challenge

6–8 weeks of ten female BALB/c mice were intramuscularly inoculated with single dose or prime-boost at a 3-week interval of VTT or deletion mutants (50 μ L). Serum samples were collected for antibody analysis two weeks after each immunization, splenocytes from five mice were harvested for T cell response analysis after the last immunization. Two weeks after the last immunization, the remaining five mice were challenged intranasally with 2.5×10^5 PFU VTT and monitored daily for weight loss and survival for 19 days following challenge. For immunization and infection, mice were anesthetized with 2% isoflurane. At the end of the experiments, mice were euthanized using 2% isoflurane, followed by cervical dislocation.

Immunization of CAST mice and MPXV challenge

20 four-week-old CAST/Eij mice were obtained from the Institute of Laboratory Animal Science, Chinese Academy of Medical Sciences. Ten mice were vaccinated intramuscularly with 1×10^5 PFU of dBTF (50 μ L), while the remaining ten mice received a negative control (PBS). Three weeks post-immunization, serum and splenocytes from five of ten mice in each group were collected for antibody and T cell response analysis. The remaining five mice of each group were then challenged intraperitoneally with 1.0×10^6 TCID₅₀ of MPXV clade IIb strain (120 μ L). Viral loads in plasma and tissues were analyzed at 4 days post MPXV infection. For both immunization and infection procedures, mice were anesthetized with 2% isoflurane. At the end of the experiments, euthanasia was performed using 2% isoflurane, followed by cervical dislocation.

Immunization of cynomolgus macaques and MPXV challenge

Six four-year-old male cynomolgus macaques were randomly divided into two groups ($n = 3$ /group) and vaccinated intramuscularly with 2.5×10^5 PFU of dBTF or a negative control (PBS, 1 mL). Monkeys were monitored daily for signs of moribundity and mortality throughout the study. Following vaccination, anesthetized physical examinations were weekly monitored. Blood samples were collected from each monkey in EDTA anticoagulant tubes. Four weeks post-vaccination, macaques were anesthetized and intravenously challenged with 4.0×10^7 TCID₅₀ of the MPXV clade IIb strain (2 mL). Skin lesions were counted at 0, 4, 7, and 10 days post-challenge. Necropsies were performed 10 days after challenge, and viral loads in the tissues and blood were analyzed by qRT-PCR or plaque assay. For immunization, blood collection, and infection procedures, the macaques were anesthetized with Zoletil 50 (5 mg/kg body weight). Euthanasia was conducted by bloodletting through the femoral artery under the condition of zoletil 50 anesthesia (5 mg/kg body weight).

ELISA of VTT, or MPXV-specific antibodies

VTT or MPXV-specific IgG antibody titers were analyzed by the enzyme-linked immunosorbent assay (ELISA). Briefly, ELISA plates were coated with 10^5 PFU heat inactivated VTT, or 1 μ g/mL MPXV M1R, B6R, H3L, A35R antigens. Serial diluted serum samples were applied to coated plates and incubated for 2 h at room temperature. After washing with PBST, the goat anti-mouse IgG-HRP (Gene-Protein Link, P03S01) or goat anti-monkey IgG-HRP antibody (Abcam, ab112767) was added to the plates. Then plates were developed by TMB substrate, and the absorbance was recorded at 450 nm using a plate reader. The end point titers of antibodies were defined as the highest dilution which reaches two times of the mean OD450 of the negative serum.

Vaccinia neutralization assay

Neutralization antibodies were measured using GFP-expressing vaccinia virus (VTT-GFP). Briefly, a serial two-fold dilution of serum samples was preincubated with VTT-GFP for 1 h at 37 °C. Then the virus-serum mixture was added to Vero cells and incubated for 24 h. The infected, GFP-expressing cells were scored using flowcytometry (BD). The neutralization titres were defined as the reciprocal of the highest dilution which reaches 50% reduction relative to the uninfected control cells.

MPXV plaque reduction neutralization assay

Plaque reduction neutralization test was performed to detect MPXV neutralization antibodies in serum samples. A serial three-fold dilution of serum samples was preincubated with 100 PFU MPXV clade IIb (MPXV-B.1-China-C-Tan-CQ01), MPXV clade Ia (MPXV-1b-China-CDC-Tan-SD01), or MPXV clade Ib (MPXV-1b-China-CDC-Tan-ZJ01) in the presence of 2.5% guinea pig serum as a source of complement (Bersee, BM361Y) for 1 h at 37 °C. Then the virus-serum mixture was added to Vero cells and incubated for 1 h. The cells were further incubated at 37 °C for 3 days and then fixed and stained with crystal violet. The PRNT₅₀ is calculated as the reciprocal serum dilution corresponding to a 50% reduction in viral plaques.

T cell response analysis

Splenocytes of immunized mice or PBMCs of macaques were harvested and analyzed for IFN- γ ELISPOT assay. ELISpot assays were performed according to the manufacturer's protocol using the mouse IFN- γ ELISpot kit (Mabtech, 3321M-4HST-2) or monkey IFN- γ ELISpot kit (Mabtech, 3421M-4HST-2). Briefly, splenocytes or PBMCs were stimulated with vaccinia specific peptides, seeded in the IFN- γ antibody coated plates, and incubated for 18–24 h at 37 °C. After washing with PBS, the plates were incubated with the detection antibody for 2 h at room temperature, and then with streptavidin-HRP for 1 h at room temperature. Substrate solution was then applied to the plate and developed until distinct spot emerges. The spots were inspected and counted using an AID ELISPOT reader system (AID Diagnostika GmbH, Strassberg, Germany).

Viral genome quantification

For viral genome quantification, vaccinia virus DNA was extracted using the QIAamp DNA Mini kit (QIAGEN) from mice organ homogenized supernatant, and analyzed by qRT-PCT using the following primers and probe targeting the *E9L* gene as previously described⁴⁵: forward primer, 5'-TGGCAAACCGTAACATACCG -3'; reverse primer, 5'-AGGCCATC-TATGATTCCATGC -3'; probe, 5'-FAM-ACGCTTCGGCTAAGAGTTGCACATCCA-TAMRA -3'. Viral genome copy number was calculated with the standard curve generated by *E9L* gene fragment-containing plasmid.

MPXV DNA was extracted from tissues of MPXV-infected animals using the Qiagen QIAamp DNA Mini extraction kit. The viral loads were determined by qRT-PCT using the following primers and probe targeting the *G2R* gene as previously described^{46–48}: forward primer, 5'-GGAAAATGTAAAGACAACGAATACAG-3'; reverse primer, 5'-GCTATCA-CATAATCTGGAAGCGTA-3'; probe, 5'-FAM- AAGCCGTAATCTA

TGTTGTCTATCGTGTCC-BHQ-1 -3'. The standard curve was generated using the plasmid DNA containing the *G2R* gene fragment. All qRT-PCR were performed and analyzed using a Bio-Rad CFX96.

Statistical analyses

Statistical differences are determined by two-tailed Student's *t*-tests between the two groups or one-way ANOVA with multiple comparison tests. Spearman correlation coefficients (*r*) are reported for binding and neutralization antibody titers with viral loads.

Data availability

Data that support the findings of this study are available within the article and as Supplementary Information. Further inquiries can be directed to the corresponding author.

Materials availability

There are restrictions to the availability of recombinant vaccinia viruses, which require a material transfer agreement for use.

Received: 11 February 2025; Accepted: 11 June 2025;

Published online: 01 July 2025

References

- World Health Organization. 2022-24 Mpox (Monkeypox) Outbreak: Global Trends. Available from: https://worldhealthorg.shinyapps.io/mpx_global/.
- US FDA. FDA Mpox Response. Available from: <https://www.fda.gov/emergency-preparedness-and-response/mcm-issues/fda-mpox-response>.
- Stittelaar, K. J. et al. Modified vaccinia virus Ankara protects macaques against respiratory challenge with monkeypox virus. *J. Virol.* **79**, 7845–7851 (2005).
- Fine, P. E., Jezek, Z., Grab, B. & Dixon, H. The transmission potential of monkeypox virus in human populations. *Int. J. Epidemiol.* **17**, 643–650 (1988).
- Jacob-Dolan, C. et al. Comparison of the immunogenicity and protective efficacy of ACAM2000, MVA, and vectored subunit vaccines for Mpox in rhesus macaques. *Sci. Transl. Med.* **16**, 27 (2024).
- Earl, P. L. et al. Immunogenicity of a highly attenuated MVA smallpox vaccine and protection against monkeypox. *Nature* **428**, 182–185 (2004).
- Earl, P. L. et al. Rapid protection in a monkeypox model by a single injection of a replication-deficient vaccinia virus. *Proc. Natl. Acad. Sci. USA* **105**, 10889–10894 (2008).
- Wolff Sagy, Y. et al. Real-world effectiveness of a single dose of mpox vaccine in males. *Nat. Med.* **29**, 748–752 (2023).
- Sanchez-Sampedro, L. et al. The evolution of poxvirus vaccines. *Viruses* **7**, 1726–1803 (2015).
- Wang, X., Gu, Z., Sheng, S., Song, R. & Jin, R. The current state and progress of mpox vaccine research. *China CDC Wkly.* **6**, 118–125 (2024).
- World Health Organization. Smallpox vaccines. Available from: <https://www.who.int/news-room/feature-stories/detail/smallpox-vaccines>.
- Kretzschmar, M., Wallinga, J., Teunis, P., Xing, S. Q. & Mikolajczyk, R. Frequency of adverse events after vaccination with different vaccinia strains (vol 3, art. no. e272, 2006). *Plos Med.* **3**, 1976–1976 (2006).
- Lane, J. M., Ruben, F. L., Neff, J. M. & Millar, J. D. Complications of smallpox vaccination, 1968. *N. Engl. J. Med.* **281**, 1201–1208 (1969).
- Monath, T. P. et al. ACAM2000 clonal Vero cell culture vaccinia virus (New York City Board of Health strain)—a second-generation smallpox vaccine for biological defense. *Int. J. Infect. Dis.* **8**, 002 (2004).
- Weltzin, R. et al. Clonal vaccinia virus grown in cell culture as a new smallpox vaccine. *Nat. Med.* **9**, 1125–1130 (2003).
- McCurdy, L. H., Larkin, B. D., Martin, J. E. & Graham, B. S. Modified vaccinia Ankara: potential as an alternative smallpox vaccine. *Clin. Infect. Dis.* **38**, 1749–1753 (2004).
- Kenner, J., Cameron, F., Empig, C., Jobs, D. V. & Gurwith, M. LC16m8: an attenuated smallpox vaccine. *Vaccine* **24**, 7009–7022 (2006).
- Tartaglia, J. et al. Highly attenuated poxvirus vectors. *AIDS Res. Hum. Retrovir.* **8**, 1445–1447 (1992).
- Wyatt, L. S., Earl, P. L., Eller, L. A. & Moss, B. Highly attenuated smallpox vaccine protects mice with and without immune deficiencies against pathogenic vaccinia virus challenge. *Proc. Natl. Acad. Sci. USA* **101**, 4590–4595 (2004).
- Frey, S. E. et al. Clinical and immunologic responses to multiple doses of IMVAMUNE (Modified Vaccinia Ankara) followed by Dryvax challenge. *Vaccine* **25**, 8562–8573 (2007).
- Meseda, C. A. et al. Enhanced immunogenicity and protective effect conferred by vaccination with combinations of modified vaccinia virus Ankara and licensed smallpox vaccine Dryvax in a mouse model. *Virology* **339**, 164–175 (2005).
- Hatch, G. J. et al. Assessment of the protective effect of Imvamune and Acam2000 vaccines against aerosolized monkeypox virus in cynomolgus macaques. *J. Virol.* **87**, 7805–7815 (2013).
- Centers for Disease Control and Prevention. Interim Clinical Considerations for Use of JYNNEOS Vaccine for Mpox Prevention in the United States. Available from: <https://www.cdc.gov/poxvirus/mpox/clinicians/vaccines/vaccine-considerations.html>.
- US FDA. Key Facts About Vaccines to Prevent Monkeypox Disease. Available from: <https://www.fda.gov/vaccines-blood-biologics/vaccines/key-facts-about-vaccines-prevent-monkeypox-disease>.
- Dalton, A. F. et al. Estimated effectiveness of JYNNEOS vaccine in preventing mpox: a multijurisdictional case-control study—United States, August 19, 2022–March 31, 2023. *Morb. Mortal. Wkly Rep.* **72**, 553–558 (2023).
- Adepoju, P. Mpox declared a public health emergency. *Lancet* **404**, e1–e2 (2024).
- Nalca, A. & Zumbun, E. E. ACAM2000: the new smallpox vaccine for United States Strategic National Stockpile. *Drug Des. Dev. Ther.* **4**, 71–79 (2010).
- Jacobs, B. L. et al. Vaccinia virus vaccines: past, present and future. *Antivir. Res.* **84**, 1–13 (2009).
- Fang, Q. et al. Host range, growth property, and virulence of the smallpox vaccine: Vaccinia virus Tian Tan strain. *Virology* **335**, 242–251 (2005).
- Parato, K. A. et al. The oncolytic poxvirus JX-594 selectively replicates in and destroys cancer cells driven by genetic pathways commonly activated in cancers. *Mol. Ther.* **20**, 749–758 (2012).
- McCart, J. A. et al. Systemic cancer therapy with a tumor-selective vaccinia virus mutant lacking thymidine kinase and vaccinia growth factor genes. *Cancer Res.* **61**, 8751–8757 (2001).
- Puhlmann, M. et al. Vaccinia as a vector for tumor-directed gene therapy: biodistribution of a thymidine kinase-deleted mutant. *Cancer Gene Ther.* **7**, 66–73 (2000).
- Buller, R. M., Smith, G. L., Cremer, K., Notkins, A. L. & Moss, B. Decreased virulence of recombinant vaccinia virus expression vectors is associated with a thymidine kinase-negative phenotype. *Nature* **317**, 813–815 (1985).
- Naik, A. M. et al. Intravenous and isolated limb perfusion delivery of wild type and a tumor-selective replicating mutant vaccinia virus in nonhuman primates. *Hum. Gene Ther.* **17**, 31–45 (2006).
- Potts, K. G. et al. Deletion of F4L (ribonucleotide reductase) in vaccinia virus produces a selective oncolytic virus and promotes anti-tumor immunity with superior safety in bladder cancer models. *EMBO Mol. Med.* **9**, 638–654 (2017).

36. El Omari, K., Solaroli, N., Karlsson, A., Balzarini, J. & Stammers, D. K. Structure of vaccinia virus thymidine kinase in complex with dTTP: insights for drug design. *BMC Struct. Biol.* **6**, 1472–6807 (2006).
 37. Slabaugh, M., Roseman, N., Davis, R. & Mathews, C. Vaccinia virus-encoded ribonucleotide reductase: sequence conservation of the gene for the small subunit and its amplification in hydroxyurea-resistant mutants. *J. Virol.* **62**, 519–527 (1988).
 38. Mayr, A., Stickl, H., Müller, H. K., Danner, K. & Singer, H. [The smallpox vaccination strain MVA: marker, genetic structure, experience gained with the parenteral vaccination and behavior in organisms with a debilitated defence mechanism (author's transl)]. *Zentralbl. Bakteriolog. B* **167**, 375–390 (1978).
 39. Hochstein-Mintzel, V., Huber, H. C. & Stickl, H. Virulence and immunogenicity of a modified vaccinia virus (strain MVA) (author's transl)]. *Z. Immunitätsforsch. Exp. Klin. Immunol.* **144**, 104–156 (1972).
 40. Eaglesham, J. B., Pan, Y., Kupper, T. S. & Kranzusch, P. J. Viral and metazoan poxins are cGAMP-specific nucleases that restrict cGAS-STING signalling. *Nature* **566**, 259–263 (2019).
 41. Hernández, B. et al. Viral cGAMP nuclease reveals the essential role of DNA sensing in protection against acute lethal virus infection. *Sci. Adv.* **6**, <https://doi.org/10.1126/sciadv.abb4565> (2020).
 42. Gammon, D. B. et al. Vaccinia virus-encoded ribonucleotide reductase subunits are differentially required for replication and pathogenesis. *PLoS Pathog.* **6**, 1000984 (2010).
 43. Mei, S. et al. Immunogenicity of a vaccinia virus-based severe acute respiratory syndrome coronavirus 2 vaccine candidate. *Front. Immunol.* **13**, <https://doi.org/10.3389/fimmu.2022.911164> (2022).
 44. Sun, H. et al. A Nuclear Export Signal Is Required for cGAS to Sense Cytosolic DNA. *Cell Rep.* **34**, <https://doi.org/10.1016/j.celrep.2020.108586> (2021).
 45. Fan, Z. L. et al. Development of a multiplex real-time PCR assay for the simultaneous detection of mpox virus and orthopoxvirus infections. *J. Virol. Methods* **328**, <https://doi.org/10.1016/j.jviromet.2024.114957> (2024).
 46. Li, Y., Zhao, H., Wilkins, K., Hughes, C. & Damon, I. K. Real-time PCR assays for the specific detection of monkeypox virus West African and Congo Basin strain DNA. *J. Virol. Methods* **169**, 223–227 (2010).
 47. Centers for Disease Control and Prevention. Test procedure: Monkeypox virus generic real-time PCR Test. Available from: <https://www.cdc.gov/poxvirus/monkeypox/pdf/PCR-Diagnostic-Protocol-508.pdf>.
 48. Porzucek, A. J. et al. Development of an accessible and scalable quantitative polymerase chain reaction assay for monkeypox virus detection. *J. Infect. Dis.* **227**, 1084–1087 (2023).
- and CIFMS 2022-I2M-CoV19-002). The funders had no role in study design, data collection and analysis, decision to publish, or preparation of the manuscript.

Author contributions

F.G., J.X., Q.W. and W.T. conceived of the project. Y.H., B.H., Z.C., J.M., L.Z., T.C. and J.L. designed the experiments. F.X., Y.H., Y.X., Z.G., C.C., J.W., J.Z. and N.L. conducted experiments. F.Z., S.M., Y.H., L.W. and L.W. designed data analysis. Y.H., Y.X., Z.G. and J.W. performed data analysis. F.X., Y.H. and J.X. wrote the manuscript. F.G., F.X. and Y.H. secured funding, administered the collaborative project, and supervised personnel.

Competing interests

F.G., F.X., Y.H. and S.M. are inventors on pending and issued patents on mpox vaccine. The remaining authors declare that the research was conducted in the absence of any commercial or financial relationship that could be construed as a potential conflict of interest.

Additional information

Supplementary information The online version contains supplementary material available at <https://doi.org/10.1038/s41541-025-01193-y>.

Correspondence and requests for materials should be addressed to Wenjie Tan, Jing Xue or Fei Guo.

Reprints and permissions information is available at <http://www.nature.com/reprints>

Publisher's note Springer Nature remains neutral with regard to jurisdictional claims in published maps and institutional affiliations.

Open Access This article is licensed under a Creative Commons Attribution-NonCommercial-NoDerivatives 4.0 International License, which permits any non-commercial use, sharing, distribution and reproduction in any medium or format, as long as you give appropriate credit to the original author(s) and the source, provide a link to the Creative Commons licence, and indicate if you modified the licensed material. You do not have permission under this licence to share adapted material derived from this article or parts of it. The images or other third party material in this article are included in the article's Creative Commons licence, unless indicated otherwise in a credit line to the material. If material is not included in the article's Creative Commons licence and your intended use is not permitted by statutory regulation or exceeds the permitted use, you will need to obtain permission directly from the copyright holder. To view a copy of this licence, visit <http://creativecommons.org/licenses/by-nc-nd/4.0/>.

© The Author(s) 2025

Acknowledgements

This study was supported by funds from the National Key R&D Program of China (2023YFC2307902), from the National Natural Science Foundation of China (82241075, 82271802, and 32200718), from CAMS Innovation Fund for Medical Sciences (CIFMS 2021-I2M-1-038, CIFMS 2022-I2M-1-021,